Methods 245 (2026) 1–12

Contents lists available at ScienceDirect

Methods

journal homepage: www.elsevier.com/locate/ymeth

Materials-Based spatiotemporal analysis of microbial responses to glyphosate in Winogradsky columns☆

Ahmad Itani [a,1,2], Marta Velaz Martín [a,1,3], Laura Meisch [a,1], Phillip Lemke [a,4], Tim Scharnweber [a,5], Islam M. Khattab [b,6], Kersten S. Rabe [a,7], Christof M. Niemeyer [a,8,*]

[a] Karlsruhe Institute of Technology (KIT), Institute for Biological Interfaces 1 (IBG-1), Biomolecular Micro- and Nanostructures, Hermann-von-Helmholtz-Platz 1, D-76344 Eggenstein-Leopoldshafen, Germany
[b] Karlsruhe Institute of Technology (KIT), Josef Göttlieb Kölreuter Institut für Pflanzwissenschaften (JKIP), Molecular Cell Biology, Fritz-Haber-Weg 4, Bldg. 30.43 D76131 Karlsruhe, Germany

ARTICLE INFO

Keywords:
Engineered polymers
Model ecosystems
Environmental microbiology
Glyphosate
Microbial dynamics
Microbial dark matter

ABSTRACT

Glyphosate, the active ingredient in many broad-spectrum herbicides, is extensively used in agriculture but has come under increasing scrutiny due to its potential impacts on non-target microbial communities. To investigate these effects within a controlled yet ecologically relevant framework, Winogradsky columns, self-contained sediment-based ecosystems, were employed as a model system. A novel, non-destructive sampling approach was introduced using macroporous elastomeric silicone foam (MESIF) integrated in stainless-steel frames to enable spatiotemporal monitoring of benthic microbial communities. These MESIF-loaded frames were vertically embedded in columns filled with lake sediment and subjected to varying experimental conditions, including light exposure and glyphosate treatment. Microbial colonization of the MESIF was assessed via amplicon sequencing at defined time points. Glyphosate-treated columns exhibited delayed microbial stratification and diminished development of characteristic pigmentation associated with functional groups such as iron-oxidizing and sulfate-reducing bacteria. Although within-column alpha diversity remained relatively constant, glyphosate exposure led to distinct shifts in community composition, including an increased abundance of taxa potentially involved in glyphosate degradation. These findings demonstrate the effectiveness of combining Winogradsky columns with MESIF-based sampling for studying environmental stressors and underscore glyphosate's influence on microbial succession and functional diversity in sediment ecosystems.

1. Introduction

Glyphosate, a phosphonic acid compound commonly marketed under the brand name Roundup™, serves as the primary active ingredient in many broad-spectrum herbicides, with global usage exceeding millions of tons annually.[1] Glyphosate is known for its effectiveness in controlling weeds by inhibiting the 5-enolpyruvylshikimat-3-phosphate synthase (EPSPS) enzyme, a key component of the shikimate pathway in plants and many microorganisms. This metabolic pathway is essential for the biosynthesis of aromatic amino acids, making glyphosate lethal to certain plant species, while largely non-toxic to animals that lack this pathway. Since its introduction in the 1970s, glyphosate has become the

☆ This article is part of a special issue entitled: 'Editors Collection - YMETH' published in Methods.

* Corresponding author.
E-mail addresses: on6879@kit.edu (A. Itani), marta.martin@kit.edu (M. Velaz Martín), laura.meisch@kit.edu (L. Meisch), tim.scharnweber@kit.edu (T. Scharnweber), islam.khattab2@kit.edu (I.M. Khattab), kersten.rabe@kit.edu (K.S. Rabe), niemeyer@kit.edu (C.M. Niemeyer).
[1] A.I., M.V.M and L.M. contributed equally to this work.
[2] https://orcid.org/0009-0001-9119-8491.
[3] https://orcid.org/0000-0002-6960-7287.
[4] https://orcid.org/0000-0002-0726-5023.
[5] https://orcid.org/0000-0001-7157-2557.
[6] https://orcid.org/0000-0003-2370-0766.
[7] https://orcid.org/0000-0001-7909-8191.
[8] https://orcid.org/0000-0002-8837-081X.

https://doi.org/10.1016/j.ymeth.2025.10.009
Received 26 June 2025; Received in revised form 24 September 2025; Accepted 25 October 2025
Available online 28 October 2025

most widely used herbicide in the world, particularly in agriculture where it is used in genetically modified glyphosate-resistant crops. However, its widespread use has raised concerns about potential environmental and health impacts, particularly regarding its effects on microbial communities, soil ecosystems, and biodiversity.[2–4] Research is increasingly focused on understanding how glyphosate affects non-target organisms, including beneficial microbes and microbial interactions within ecosystems. With growing concern over glyphosate's effects on the potential disruption of microbial communities, researchers are seeking model systems to study these effects in detail. One such model is the Winogradsky column, a self-contained, layered microbial ecosystem designed to simulate natural environmental conditions. These columns, named after the Russian microbiologist Sergei Winogradsky, [5] are typically filled with sediment, water and nutrients and provide a controlled but dynamic environment for the study of microbial diversity, metabolic activities and ecological interactions. Because they contain a diverse array of microbial communities engaged in complex interactions, Winogradsky columns provide a unique, accessible platform for studying how microbial communities self-organize to sustain the carbon cycle or how they respond over time to external factors, such as herbicides like glyphosate.[6–8].

While modern sequencing methods have recently improved our understanding of the spatial and temporal distribution of microbial communities in Winogradsky columns,[9] these approaches remain limited to endpoint measurements, as sequencing analysis can only be performed after the physical disruption of the microbial ecosystem. To overcome these limitations, we present a novel approach originally developed for sampling microbial communities from various habitats, which relies on the use of bioinert porous materials systems. Recently, we reported the development and application of innovative devices that integrate a matrix of macroporous elastomeric silicone foam (MESIF) into a simple, scalable chip design.[10] MESIF can be fabricated in bulk as a biomimetic foam material from polydimethylsiloxane (PDMS) using a straightforward procedure. This system was applied to explore the "microbial dark matter" (MDM) within environmental microbiomes obtained from diverse habitats, ranging from moist, turbulent biofilters and wastewater treatment plants to dry, air-based environments.[10] In these settings, the porous MESIF material proved highly effective for supporting efficient microbial colonization simply by being placed in contact with the respective habitats. Moreover, MESIF enabled robust isolation of DNA from the associated microbial communities, and the extracted DNA consistently showed the quality required for downstream sequencing. Notably, this initial study also revealed that rare microorganisms associated with MDM were efficiently enriched within the porous matrix of MESIF. Building on these findings,[10] which provided detailed insights into community composition, we hypothesized that the MESIF materials may also be suitable for spatiotemporal analyses of microbial community dynamics within the closed system of a Winogradsky column. We further reasoned that this approach could enable the capture of temporal dynamics in benthic microbial communities, that is, communities of microorganisms living in aquatic sediments. These microbial communities play a crucial role in the biogeochemical cycle by breaking down organic matter, recycling nutrients, and contributing to the stability of the ecosystem.

To enable a spatiotemporal analysis of a benthic community in a Winogradsky column, we arranged MESIF pieces longitudinally within a steel frame, which served as a support to position the MESIF pieces vertically within the layered structure of the Winogradsky column (Fig. 1). Three such MESIF-loaded frames were then positioned in a plexiglass cylinder and overlaid with fresh sediment from a local freshwater lake to initiate the development of the typical layered structure of a Winogradsky column. At various time points, individual

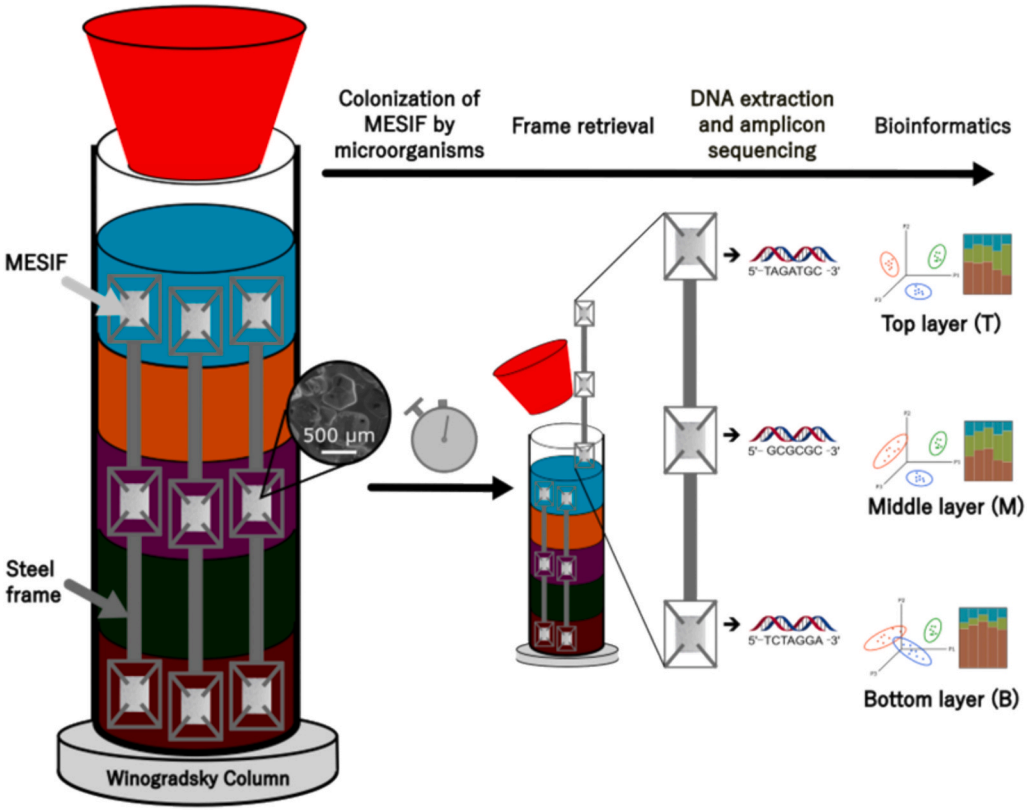

Fig. 1. Strategy for spatiotemporal sampling of Winogradsky columns using MESIF pieces. MESIF pieces are held at fixed heights within the layered structure of a Winogradsky column using steel frames. During the development of the column, microorganisms colonize the MESIF material. The photographic inset shows the typical structure of the macroscopic pores in the MESIF material. At specific time points, individual frames are removed, and the corresponding MESIF pieces are processed for DNA extraction to determine the identity and abundance of the contained microorganisms.

frames could be removed from the sediment to analyze the microbes that had colonized the MESIF using sequencing techniques. Different experimental conditions were applied during the maturation of the Winogradsky columns, including variations in light exposure (presence or absence of light) and the presence or absence of glyphosate to study its effect on microbial community development. We aimed to characterize the microbial communities present in the upper, middle, and lower layers of the Winogradsky columns, with a particular focus on assessing the impact of glyphosate on their biodiversity. We found that glyphosate-treated columns showed delayed stratification and slower development of pigmentations associated with iron-oxidizing and sulfate-reducing bacteria. While overall biodiversity within individual columns was similar, there was a clear difference in diversity between glyphosate treated and untreated columns, with an increase in potentially glyphosate-degrading bacteria in the treated columns.

2. Materials and methods

2.1. MESIF fabrication

The MESIF were fabricated according to a previously published protocol[10] with minor modifications. In brief, a polydimethylsiloxane (PDMS) solution was prepared by mixing prepolymer solution with curing agent (Sylgard 184, Down Corning) in a 10:1 ratio by mass. After degassing for 30–45 min in a vacuum chamber, the solution was poured into a mold fabricated from polymethylmethacrylate (PMMA). Table salt, sieved to obtain only grains (porogens) of diameters 500–700 μm, were then poured on top of the PDMS solution in the mold. To ensure homogenous dispersion of the grains in the prepolymer solution, the mold was centrifuged at 4600 rpm and 4 °C for 20 min (5804R, Eppendorf). The resulting mixtures were then cured in an oven (Heraeus, Thermo Scientific Inc.) at 70 °C for an hour. After removal from the molds, the resulting MESIF pieces were placed in double-distilled water in a mechanical stirrer overnight to facilitate leaching of the porogen crystals from the materials. The MESIF were then cut into pieces of 10 x 10 x 3 mm^3 each.

2.2. Fabrication of steel frames

In order to fix the MESIF to specific heights within the columns, frames were designed using Autodesk Inventor 2020 (Autodesk Inc.) for use as support structures to hold the MESIF in place. The frames were fabricated from stainless-steel with thickness 0.5 mm using a HL62P laser cutter (Trumpf HAAS Laser) at the Institute for Astroparticle Physics at KIT. To ensure simplicity and reusability, the frames were designed with sharp corners protruding from the edges that fold into a square window (Fig. S1). The sponges can thus be pierced by the corners to fix them on a specific height.

2.3. Sediment collection and post processing

Samples of mud were collected on March 1st 2022 from multiple spots of a local freshwater lake in Saalbachniederungen Hambrücken (49.1557, 8.5469). The samples were sieved using a 6 mm soil sifter to remove stones and debris, and subsequently pooled and homogenized to ensure a broader representation of the diverse taxa present in the lake. By relying on a single, well-defined collection date, external variability due to seasonal changes in community composition was minimized, thus providing consistent starting material across all experimental conditions. To estimate the amount of sediment required to achieve a 1 % (w/w) glyphosate concentration, the water content of the samples was determined. 9 samples were isolated on weighing dishes, weighed once before drying, then left to dry for 24 h in a B5042 incubator (Heraeus Group) at 70 °C. Their mass was measured using a Kern EMB-V precision balance (Kern Ltd.) at different time points showing that after 24 h no more evaporation was taking place (values in Table 1). The resulting average dry-to-fresh weight ratio of 38.2 % was used to estimate the mass of dry sediment during the experiment and to calculate the amount of glyphosate needed to achieve a 1 % (w/w) concentration. Unused sediment was frozen in bottles at −80 °C.

Table 1
Masses of sediment samples before and after drying, and the calculated ratio of dry to starting fresh sediment in %.

Sample No.	Starting Mass (g)	After 12 h drying	After 24 h drying	% Dry sediment
1	30	11.2	11.2	37.3
2	30	11.1	11.1	37
3	30	10.9	10.9	36.3
4	30	11.2	11.2	37.3
5	30	11	11	36.7
6	20	7.7	7.7	38.5
7	20	8.1	8.1	40.5
8	40	16.2	16.2	40.5
9	40	15.8	15.8	39.5

2.4. Assembly of Winogradsky columns

Columns were constructed using 20 cm long polymethyl methacrylate (PMMA) tubes with an inner diameter of 4 cm. The bottom of each column was sealed with a hexagonal PMMA plate using a hot glue gun. Rubber stoppers (MOCAP) were used to act as air-tight lids closing the columns (Fig. S2). As some of the columns were intended to contain glyphosate, and each of the eight columns was to be filled with 200 mL of slurry, the original sample was divided into two equal portions: 800 mL of unaltered slurry and 800 mL to be amended with glyphosate. The glyphosate-treated portion weighed approximately 768 g and was estimated to contain 293.4 g of dry sediment. To achieve a 1 % (w/w) glyphosate concentration, 3 g of powdered glyphosate (Molekula) was added. The assembly of the Winogradsky column followed a previously reported procedure.[9] In order to boost the formation of a sulfide gradient and accelerate the segregation of microorganisms, the columns were filled at the bottom with enriched sediment as described before.[9] To this end, the samples were further split into slurries enriched with 4.5 g dried leaf litter, 5 g $CaSO_4$, and 5 g $CaCO_2$ per 100 mL sediment. The result was four mixtures: 1. Unenriched sediment, 2. Enriched sediment, 3. Unenriched sediment with 1 % (w/w) glyphosate, and 4. Enriched sediment with 1 % (w/w) glyphosate. To set up the experimental columns, each was first filled with 50 mL of enriched sediment (reaching a height of 4 cm), followed by the insertion of the MESIF-loaded holders. The columns were then topped up with 150 mL of unenriched sediment (up to 16 cm) to fully cover the MESIF and subsequently sealed with a rubber stopper. Each column therefore contained 200 mL of sediment. We established four different types of columns: (1) with 1 % (w/w) glyphosate and exposed to light, in the following referred to as "+G+L", (2) with glyphosate and wrapped in aluminum foil to cover from light irradiation (+G-L), (3) without glyphosate and exposed to light (-G+L), and (4) without glyphosate and wrapped in aluminum foil (-G-L).

2.5. Incubator

A 90x72x55 cm chamber (Fig. S3A) was built and augmented with 3 LED lamps (SOLAR STINGER®, ECONLUX, 25 W each) each 72 cm in length in order to provide illumination for the columns. The lamps were each 25 cm apart. The incubator is open from the top in order to allow for observation of the columns. Representative images are shown in Fig. S3B. The walls of the incubator were covered with aluminum foil to provide as much thermal insulation as possible. The lights were controlled by the con1 control unit provided by ECONLUX, and the setting used was SOLAR STINGER® SunStrip III 35 FRESH. The Winogradsky columns were incubated under constant illumination.

2.6. MESIF retrieval

To ensure consistent sampling, the MESIF-holder frames were systematically retrieved from the individual Winogradsky columns at specific time points. On day 20, the columns were opened, and the frames were carefully removed. The corresponding MESIF pieces were extracted from the frames by carefully unfolding the frames and detaching the MESIF from the sharp corners using tweezers sterilized with isopropanol, and placing them in Eppendorf Tubes. The tubes were then stored at −80 °C. To maintain continuity, new MESIF-loaded frames were inserted into the columns on day 30. These replacement frames were then retrieved on days 72 and 109, resulting in MESIF incubation periods of 42 and 72 days inside the Winogradsky columns, respectively. In some cases, MESIF pieces slipped out of the frames and were lost within the column during retrieval. This occurred with the B-MESIF piece (located at the bottom) of the -G-L column on day 72 and the B pieces retrieved from the +G+L columns on days 72 and 109. Additionally, any middle MESIF pieces that had protruded from the sediment and been exposed to water rather than sediment were excluded from further analysis to avoid inconsistencies in environmental exposure.

2.7. Sequencing and bioinformatic analysis

MESIF pieces were rinsed with autoclaved deionized water to remove adhering sediment and subsequently cut into two pieces. Genomic DNA (gDNA) was extracted from only one of the pieces with DNeasy Power soil Soil Pro Kit (Qiagen GmbH, Germany). In addition to the protocol provided by the manufacturer, the MESIF were squeezed with sterile tweezers in the lysis buffer in order lyse the microorganisms inside of the pores. Quantification of gDNA was always performed by measuring the fluorescence of a DNA intercalating dye using the Qubit 3 instrument (Thermo Scientific Inc, Germany).

For amplicon sequencing the V3 region of the 16S rRNA was amplified with the degenerated primers 341bf (ACACTCTTTCCCTACACGACGCT CTTCCGATCTCCTACGGGNGGCWGCAG) and 518r (GACTGGAGTTCA-GACGTGTGCTCTT CCGATCTWTTACCGCRGCTGCTGG), which already included the TruSeq adapters for Illumina sequencing. The PCR reactions were performed with 0.04 U/μL High-Fidelity Q5 DNA Polymerase, 1 × Q5 reaction buffer, 1 × high GC enhancer, 0.25 μM of each primer, 0.2 mM dNTPs, and 100 ng template DNA with 25 μL total reaction volume. The PCR was performed with a touchdown protocol cycling trough the following conditions: 95 °C, 2 min; 4 x (95 °C, 9 s; 56–52 °C, 40 s; 72 °C, 40 s); 25 × (95 °C, 40 s; 51 °C, 40 s; 72 °C, 40 s); 72 °C, 5 min and hold at 4 °C). The amplified DNA was purified using the DNA Clean and Concentrate-25 Kit (Zymo Research, USA). To construct indexed sequencing libraries, samples were cleaned up by a size selection with AMPure XP Beads (Beckmann Coulter USA), followed by a 6-cycle index PCR step using Unique dual indices (NEB, Germany). Verification of library quality was done using the Agilent 2100 Bioanalyzer (Agilent Technologies, Germany) with the Agilent Hight Sensitivity DNA Kit. Sequencing was performed with an Illumina NextSeq 1000 (Illumina, USA) with the NextSeq 1000/2000 P1 Reagents kit (300 Cycles) (Illumina, USA) generating paired end reads.

Sequences were analyzed using QIIME 2 (version 2021.8.0, an open-source microbiome bioinformatics platform).[11] The demultiplexed was denoised with DADA2[12] using q2-dada2 to generate amplicon sequence variants (ASVs). The ASVs were aligned with mafft via q2-alignment[13] and used as basis for the construction of the phylogeny with fasttree 2[14] via q2-phylogeny. Alpha and beta diversity was calculated in R with the qiime2R[15], phyloseq[16] and the microbiome package.[17] For alpha diversity and Shannon diversity and Faith PD Indexes were calcutated. Beta Diversity was calculated based on Weighted Unifrac, Jaccard Distace and Bray-Curtis dissimilarity. Taxonomic classification was assigned to the ASVs with the q2-feature-classifier[18] using the classify-sklearn naive Bayes taxonomy classifier against the Silva 138 SSURef NR99 full-length taxonomy database.[19] Differential abundance testing was performed using Analysis of Composition of Microbiomes with Bias Correction (ANCOM-BC)[20] in R. ANCOM-BC estimates log-fold changes (LFCs) in taxon abundance relative to a specified reference group (in this study, the -G+Lgroup), while accounting for the compositional nature of microbiome data and correcting for sequencing depth biases. Statistical significance of the estimated LFCs was evaluated using the Wald test. To control for multiple hypothesis testing, p-values were adjusted using the Benjamini–Hochberg procedure, a standard approach for controlling the false discovery rate in high-dimensional microbiome datasets. Taxa with adjusted p-values below 0.05 were considered significantly differentially abundant. For visualization purposes, LFC values corresponding to non-significant taxa were masked (set to NA), ensuring that only statistically supported differences were displayed in the results.

2.8. Replication and sampling strategy

For each condition and timepoint, two Winogradsky columns were prepared (n = 2), yielding biological duplicates. Each retrieved frame contained three identically sized MESIF pieces (10 × 10 × 3 mm), enabling spatially resolved sampling from the top, middle, and bottom sections of the columns. This standardized design ensured comparability of samples across depths and timepoints. Although some MESIF pieces were lost during handling, resulting in occasional single-sample data points, the overall workflow provided reproducible spatiotemporal resolution of community dynamics. Statistical analyses were limited to ANCOM-BC for differential abundance testing, while alpha- and beta-diversity metrics are presented descriptively due to the restricted sample size.

3. Results and discussion

3.1. Experimental workflow

To investigate the spatial separation and temporal dynamics of microbial communities in Winogradsky columns, we designed a modular sampling system based on macroporous MESIF pieces, prepared as previously described [10] and mounted in steel frames (Fig. 2). To this end, the as prepared MESIF piece (Fig. 2A) was cut into smaller pieces (~10 x 10 x 3 mm^3, Fig. 2B) and mounted into a steel frame (Fig. 2C; technical drawing in Fig. S1). This support element consisted of four square subframes, each featuring folding tabs at the corners that could be bent to act as clamps, securing the MESIF pieces in place (Fig. 2D). Minor inhomogeneities between Winogradsky columns prevented placement of two MESIF pieces in the middle section, so all analyses were performed with support frames containing three pieces. This setup enabled systematic sampling of defined positions along the vertical gradient of the columns: top (aerobic), middle (transition), and bottom (anaerobic). Importantly, each retrieved frame contained three identically sized MESIF pieces, ensuring that samples from different depths were directly comparable in size and structure. By standardizing both the sampling geometry and material properties, this approach reduced variability between replicates and allowed reproducible assessment of community dynamics across time points.

Up to three MESIF-loaded holders (Fig. 2D) were arranged in a transparent cylinder of polymethyl methacrylate (PMMA, see also Fig. S2) and carefully overlaid with the materials for the Winogradsky column as detailed in sections 2.3 and 2.4 (Fig. 2E-G). The MESIF-loaded frames could be removed from the columns without substantially disturbing the sediment structure, which provided a clear spatial resolution of microbial communities while maintaining the integrity of the system. Over the course of the experiment (days 20, 72, and 109), this design allowed us to trace microbial succession at multiple depths, highlighting how aerobic and anaerobic zones shaped community composition. Furthermore, since biomass consistently accumulated within the porous MESIF, samples across all positions and time points yielded DNA of

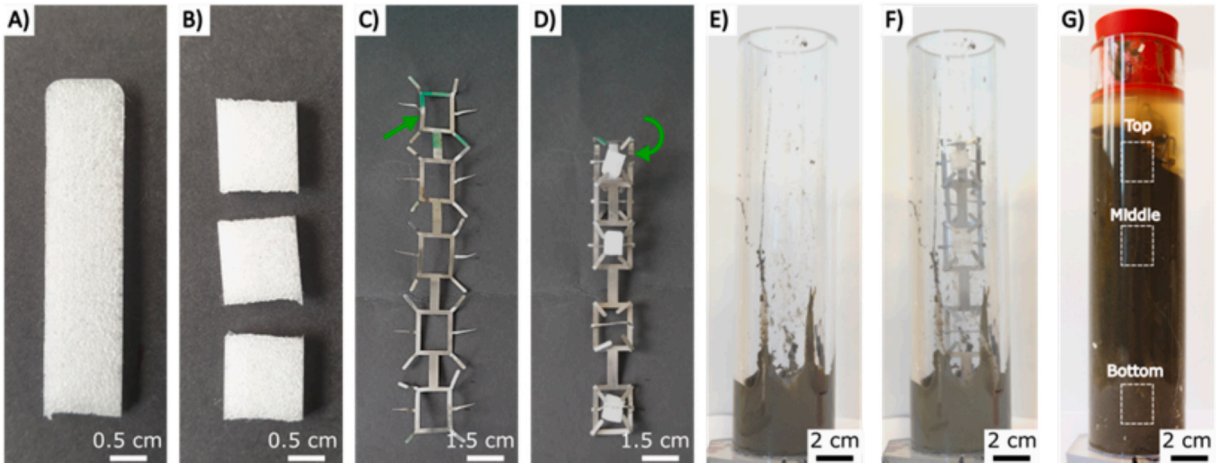

Fig. 2. Workflow to assemble columns with MESIF pieces positioned at three fixed heights. A) Large pieces of MESIF, made of PDMS-NaCl porogen dispersions, were cut into smaller pieces of ~ 10 x 10 x 3 mm^3. These pieces (B) were mounted in a steel frame holder (C) that consisted of five square subframes. Each subframe included folding tabs at the corners that could be bent to function as clamps. The entire frame was designed to be flexibly bent in order to adapt the MESIF pieces to varying column heights. Note that in the example shown, the upper MESIF holder (green arrow) was bent backward, shortening the frame from five to four subframes, and allowing the secure positioning of three MESIF pieces within the sediment column (D). E) Enriched benthic sediment was added to the bottom of an empty transparent PMMA cylinder, and up to three MESIF-loaded holders were positioned within it (F). The setup was then topped off with unenriched sediment. Note that each holder contained three MESIF pieces, allowing for sampling from the top, middle, and bottom sections of the stratified Winogradsky columns (G) upon removal of a single holder. The dashed squares indicate the positions of the MESIF. Scale bars are 0.5 cm (A, B), 1.5 cm (C, D) and 2 cm (E-G). (For interpretation of the references to colour in this figure legend, the reader is referred to the web version of this article.)

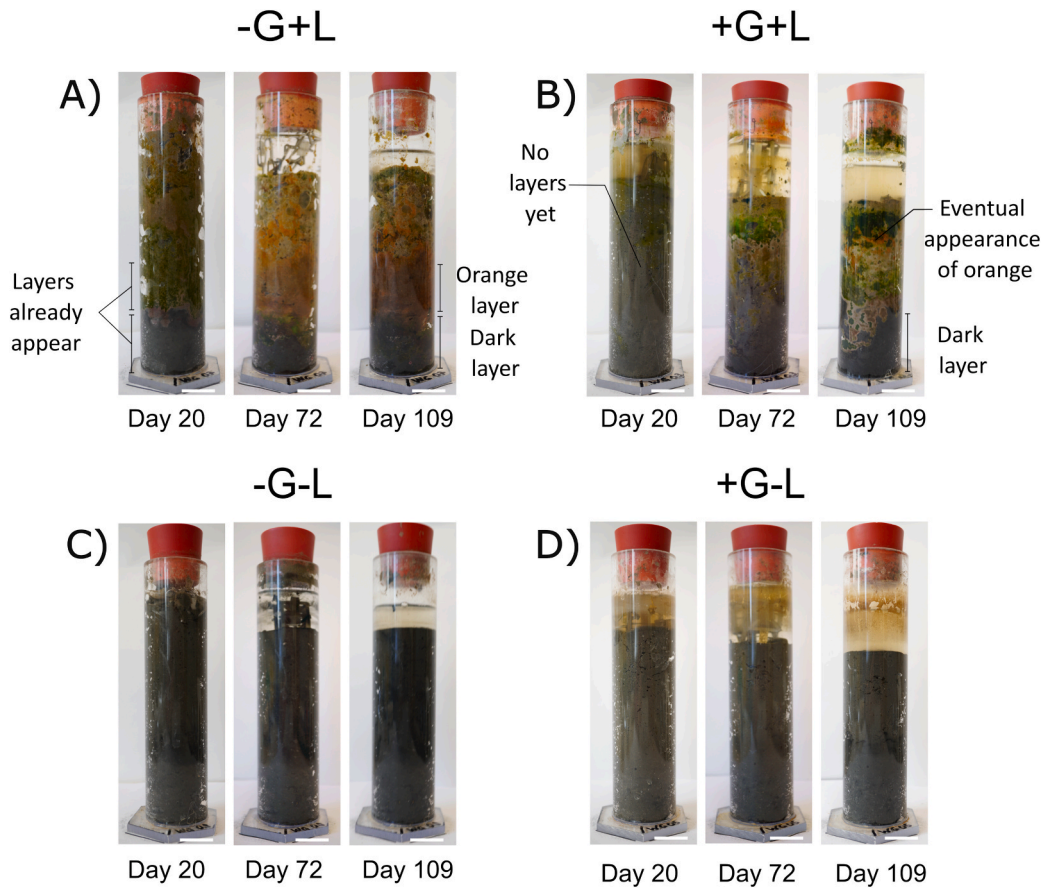

Fig. 3. Representative photographs of Winogradsky columns. The images shown here were taken on the days of MESIF holder retrieval: (A) columns without glyphosate and exposed to light (-G+L), (B) columns with glyphosate and exposed to light (+G+L), (C) columns without glyphosate and kept in darkness (-G-L), and (D) columns with glyphosate and kept in darkness (+G-L). Photographs of the replicates of these columns are shown in Fig. S4. All scale bars are 20 mm.

comparable quantity and quality, supporting robust downstream sequencing analyses.

In addition to spatially resolved sampling, reproducibility was enhanced by preparing eight parallel Winogradsky columns under controlled conditions that differed only in glyphosate exposure and light regime. This ensured that observed community shifts could be attributed to treatment effects rather than technical inconsistencies. Overall, the integration of MESIF matrices into the Winogradsky system provided a reliable platform for resolving vertical gradients and temporal changes in microbial ecology with high reproducibility.

3.2. Visual observations during the development of Winogradsky columns

To investigate the influence of glyphosate on microbial communities, we prepared columns with and without 1 % (w/w) glyphosate, which corresponds to concentration range found for working solutions in commercial herbicide formulations and was chosen to allow realistic exposure.[21] To simulate the effect of increasing soil depth and reduced light exposure, we also prepared replicate columns covered with aluminum foil to mimic the deeper dark layers of natural sediment. Based on this setup, we established four different types of columns: (1) with 1 % (w/w) glyphosate and exposed to light (+G+L), (2) with glyphosate and wrapped in aluminum foil (+G-L), (3) without glyphosate and exposed to light (-G+L), and (4) without glyphosate and wrapped in aluminum foil (-G-L), see also Fig. S2. Two replicates of each type were prepared, resulting in a total of eight columns. The columns were incubated for several months under continuous 24-hour light exposure in an incubator equipped with artificial lighting. To monitor the development and stratification of microbial communities over time, photographs were taken weekly to capture observable spatiotemporal changes, particularly in sediment coloration, which reflects shifts in bacterial activity and the formation of distinct layers. Representative photographs taken on the days when frames were retrieved are shown in Fig. 3.

Given the opacity and heterogeneity of Winogradsky columns, spectrophotometric methods are not feasible for non-destructive monitoring. Consistent with established practice in Winogradsky research,[9] we therefore present a qualitative assessment based on visual inspection supported by photographic documentation, which may in future be complemented by quantitative image analysis. Based on these observations, the development of the columns can be cautiously divided into three phases: a stratification phase, a maturation phase, and a post-maturation phase, represented by days 20, 72, and 109, respectively. These time points were chosen to provide the incubated MESIFs sufficient time to adapt to the changing column conditions and thereby more reliably reflect microbial dynamics.

The visual inspection revealed that by day 20, as shown in the photographs in Fig. 3, the columns exposed to light without glyphosate (-G+L, Fig. 3A) developed dark bottom layers characteristic of sulfate-reducing bacteria, which were not observed in the corresponding glyphosate-treated columns (+G+L, Fig. 3B). However, by day 72, both types of columns had developed similarly well-defined stratification. At this point, the -G+L column (Fig. 3A) displayed a prominent orange pigmentation indicative of iron-oxidizing bacteria,[9] which was less pronounced in the +G+L column (Fig. 3B). By day 109, the layering in the -G+L column (Fig. 3A) remained relatively unchanged compared to day 72. In contrast, the orange pigmentation in the +G+L column (Fig. 3B) had increased substantially. Similar patterns were observed in the corresponding replicates (Fig. S4B). The delayed appearance of orange pigmentation in the +G+L columns may be attributed to glyphosate's role as a metal chelator.[22,23] Glyphosate-mediated chelation of iron could have inhibited the formation of iron oxides, which are responsible for the characteristic orange color.[9] Furthermore, it is known from environmental studies that transcription of genes related to iron acquisition and metabolism can be significantly downregulated in the presence of glyphosate.[24] However, the eventual emergence of iron oxide-related pigmentation suggests that glyphosate was ultimately degraded, allowing iron to become available once again to iron-oxidizing taxa. In contrast to their illuminated counterparts, the -L columns (Figs. 3C and 3D) did not exhibit any clear stratification.

Visual observations strongly indicated that glyphosate distinctly influences microbial communities, as evidenced by the differing pigmentation patterns between treated and untreated columns. These differences suggested that glyphosate may affect both the onset and progression of microbial activity within the system. This supported the suitability of Winogradsky columns as an experimental model for investigating glyphosate's effects on microbial ecosystems. To gain deeper insight into the spatiotemporal dynamics of these communities, additional sequencing analyses were conducted.

3.3. Sequencing-based assessment of condition-dependent microbiome diversity

To further analyze the microbial communities in the Winogradsky columns, MESIF-loaded holders were retrieved from the respective columns on days 20, 72, and 109. Genomic DNA (gDNA) was then extracted from the MESIF pieces positioned at the lower and middle levels using a commercial reagent kit (DNeasy Power Soil Pro Kit, Qiagen, Germany). For amplicon sequencing the V3 region (314 – 518) of the 16S rRNA was amplified with primers added to Illumina TrueSeq Adapters. After library preparation the samples were sequenced on an Illumina NextSeq1000 instrument. The bioinformatic analysis of the sequences was conducted using QIIME2 (v2021.8.0),[25] with diversity matrices calculated via the q2-diversity plugin.

The placement of MESIF pieces at the top position (T) within the columns was originally intended to enable the analysis of microbial communities at the water–sediment interface. However, during the experiment, sediment compaction led to the formation of a supernatant layer that consistently exposed the top MESIF to an aquatic environment (Fig. S5). Sequencing data revealed a disproportionately high abundance of *Cyanobacteriota* in MESIF pieces either adjacent to (position M) or directly exposed to the supernatant (position T), as shown in Fig. S5. While the high presence of phototrophs in this niche is biologically relevant, their dominance complicated the comparative analysis of broader microbial diversity across experimental conditions. To avoid confounding effects in the interpretation of treatment responses, all top-position MESIF samples were excluded from further analysis. When examined separately, however, the alpha diversity of samples at the water–sediment interface showed no systematic differences between conditions, with consistently high values across all treatments (Fig. S6A–B). In contrast, beta diversity analyses (Fig. S6C–E) revealed that communities from glyphosate-treated columns, particularly under light exposure (+G+L), were more dispersed than those without glyphosate, indicating greater instability and variability in community composition.

To evaluate how microbial diversity is affected by glyphosate and light exposure, we first compared alpha diversity at various time points within each column and across all conditions, based on bioinformatic analysis of the sequencing data. As there were no significant differences in alpha diversity, the data from the B and M layers were grouped and not shown separately in subsequent analyses. Alpha diversity measures the biodiversity within individual samples, providing insights into species richness and evenness.[26,27] Shannon diversity quantifies species richness and evenness within each sample, while Faith's Phylogenetic Diversity (Faith PD) incorporates phylogenetic relationships, accounting for evolutionary distances between species. Across all conditions, both diversity measures increased over time, with the lowest diversity observed at day 20 (red bars in Figs. 4A, 4B). As time progressed, the microbiome in the Winogradsky columns became more diverse (Figs. 4A, 4B, green, blue). However, alpha diversity remained consistent across conditions, indicating that neither glyphosate exposure nor illumination had a significant effect on within-sample biodiversity.

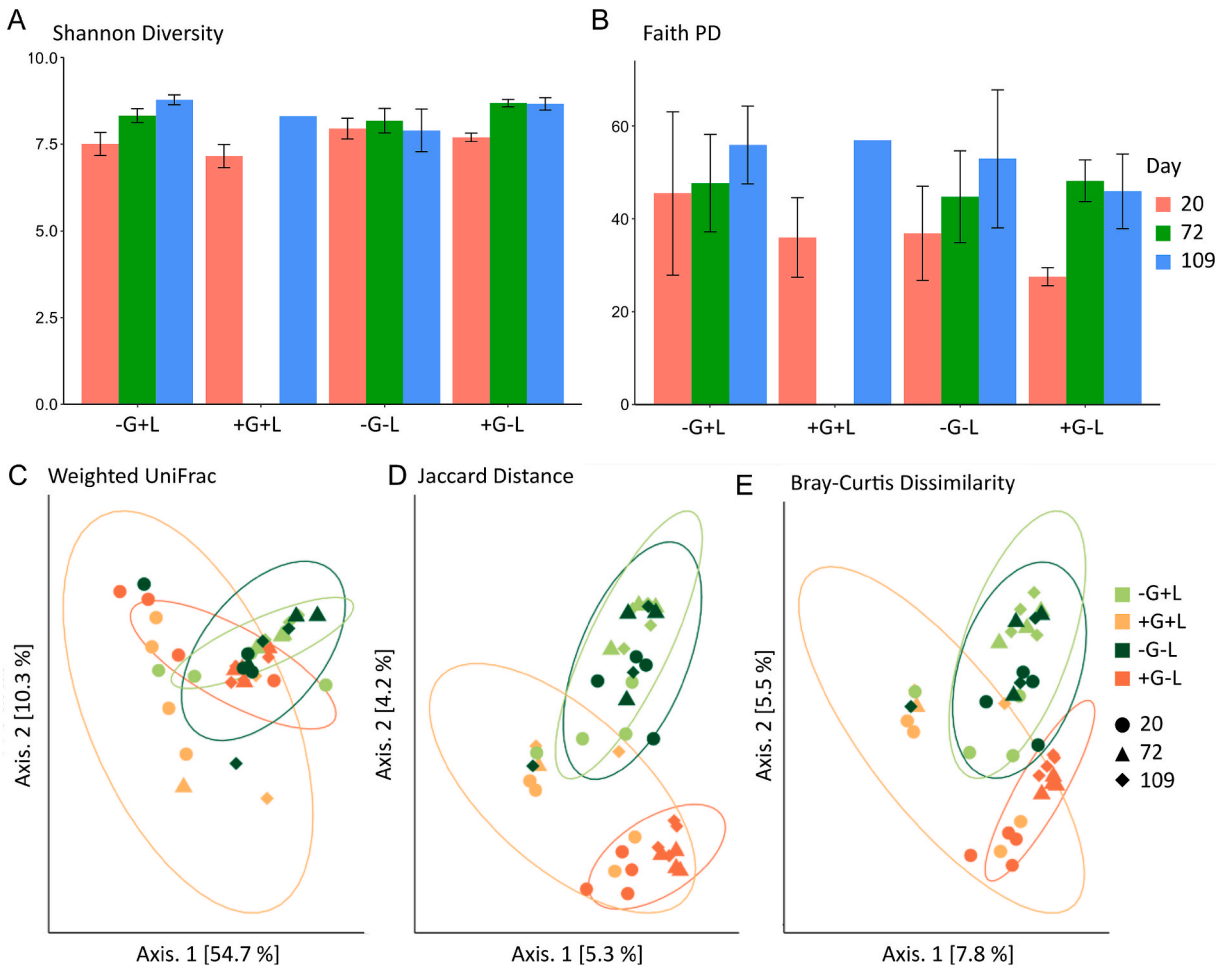

Fig. 4. Alpha and beta diversity of the microbiome within the MESIF, derived from their respective columns. Alpha diversity is represented by Shannon entropy (A) and Faith's PD (B) across four conditions: -G+L, +G+L, -G-L, and +G-L. MESIF pieces from Winogradsky columns were retrieved at day 20, day 72, and day 109. Due to unforeseen experimental complications, samples from the +G+L column on day 72 could not be recovered for analysis. Beta diversity is shown using Weighted Unifrac (C), Jaccard Distance (D), and Bray-Curtis Dissimilarity (E). The four conditions -G+L (light green), +G+L (orange), -G-L (dark green), and +G-L (red) are enclosed within ellipses representing 95 % confidence regions, assuming a multivariate normal distribution. Sampling timepoints are indicated by circles (day 20), triangles (day 72), and diamonds (day 109) and contain both B and M MESIF pieces. Fig. S7 shows a similar beta diversity analysis to determine the influence of using parafilm instead of rubber stoppers to cover the columns. (For interpretation of the references to colour in this figure legend, the reader is referred to the web version of this article.)

To quantify differences between microbial communities across the various Winogradsky samples and identify patterns of community variation, we also assessed so-called beta diversity.[26,27] Therein, several distance metrics provide different perspectives on community composition. The Jaccard Distance considers only species presence or absence, while Bray-Curtis Dissimilarity incorporates species abundance and Weighted UniFrac further integrates phylogenetic relationships into the comparison. We found that both Jaccard Distance and Bray-Curtis Dissimilarity revealed similar beta diversity patterns. Winogradsky columns developed in the absence of glyphosate, regardless of illumination, clustered closely together particularly in later sampling days (Figs. 4D, 4E, light and dark green circles). In contrast, the introduction of glyphosate as a stressor shifted communities further apart (Figs. 4D, 4E, orange and yellow). Notably, the glyphosate-treated non-illuminated column (+G-L, red circle) formed a distinct cluster with a visible shift between day 20 and later timepoints. In contrast, the glyphosate-treated illuminated column showed the greatest dispersion, as indicated by the largest confidence interval ellipse (Figs. 4D, 4E, +G+L orange). A similar pattern was observed in the Weighted UniFrac analysis, where the +G+L condition exhibited no big clustering (Fig. 4C, orange). Generally, while non-stressed columns clustered together, the glyphosate-treated non-illuminated column also aligned with this group, suggesting a less pronounced effect of glyphosate in the absence of light. Notably, the analysis of three beta diversity metrics revealed no significant clustering between MESIF pieces positioned in the bottom versus middle regions of the Winogradsky columns, irrespective of the cultivation conditions (Fig. S8). This lack of spatial separation suggests that, under the given experimental parameters, microbial communities in these two sediment depths were either highly similar or influenced more strongly by overarching environmental factors, such as substrate composition or nutrient gradients, than by vertical positioning alone.

In natural environments, soil and sediment are typically devoid of light. In this study, illumination did not significantly alter the microbial composition within the MESIF of columns without glyphosate, suggesting that the microbial community was resilient to potential disturbances caused by light exposure. However, in the +G-L condition, glyphosate alone induced a shift in the microbial community, but the composition remained relatively stable over time (compare dark green -G-L vs red +G-L, in Fig. 4C-E). In contrast, the +G+L condition (showed the highest community instability, with greater divergence among samples from different time points (see orange circles, in Fig. 4C-E). This instability may be due to the combined effects of glyphosate and illumination and might be linked to known molecular effects of glyphosate. It inhibits the shikimate pathway by targeting the EPSPS (5-

enolpyruvylshikimate-3-phosphate synthase),[28] a mechanism that affects a wide range of organisms including plants, fungi, bacteria or algae.[29] Because we performed 16S rRNA amplicon sequencing, we were only able to assess bacterial community compositions and lack information about potential eukaryotic responses. Within bacteria, some taxa can tolerate glyphosate through resistant EPSPS variants[30] or by metabolizing glyphosate as a phosphorous source via enzymes such as C-P lyase or glyphosate oxidoreductase.[31] In illuminated conditions, inhibition of sensitive phototrophs could reduce community stability and open ecological niches for opportunistic taxa. This might contribute to the increased variability we observed. While our data cannot directly resolve these mechanisms, they provide a plausible framework for interpreting the community-level instability under +G+L. Taken together, the results indicate that our approach is well suited to track temporal shifts in microbial communities within the columns and to sensitively reflect the impact of environmental factors, including light and the chemical stressor glyphosate.

3.4. Taxonomic classification of the microbial communities

To gain deeper insights into the observed shifts in microbial composition and stability, we next performed a taxonomic classification of the microbial communities. To characterize the microbial taxonomy within the columns, amplicon sequence variants (ASVs) were taxonomically classified using the q2-feature-classifier plugin,[18] with reference to the SILVA 138.1 SSU database.[19] The relative abundances of microorganisms detected in MESIF pieces positioned at different heights within the differently treated Winogradsky columns were calculated and visualized as bar plots at the phylum level (Fig. 5).

The taxonomy assessment results indicated that the microbial community within the Winogradsky columns remained generally stable, with only minor variations observed within each condition. A comparison of MESIF pieces positioned at the bottom (B) and middle (M) levels of the columns revealed no significant shifts, suggesting that the position within the column had no clear effect on microbial composition. However, distinct differences in phylum-level abundances were observed between different treatment conditions. In the presence of glyphosate, *Acidobacteriota* decreased, while *Bacillota* and *Bacteroidota* increased, indicating that glyphosate selectively influences microbial community composition (Fig. 5).

Interestingly, *Patescibacteria* — part of the Candidate Phyla Radiation (CPR), a diverse group of bacteria with small genomes and limited metabolic capabilities — were primarily detected in the absence of glyphosate, suggesting that this group is unable to tolerate glyphosate exposure. In contrast, *Chloroflexota* showed a gradual increase over time, particularly in the presence of glyphosate, consistent with their classification as slow-growing organisms, especially members of the class *Anaerolineae*.[32,33] This pattern may indicate tolerance or indirect ecological benefits rather than active degradation. Additionally, this trend underscores the advantage of using materials like MESIF, which support a broader community distribution and prevent dominant phyla from outcompeting others, as previously shown.[10] In untreated illuminated Winogradsky columns (-G+L), *Chloroflexota* exhibited only a minor increase in abundance over time, which was less pronounced compared to glyphosate-treated columns. This suggests that glyphosate may act as a stressor for *Chloroflexota*, initially hindering their growth. However, glyphosate was likely degraded over time, possibly by other microbial groups indigenous to soil as seen in previous studies. Diverse bacterial taxa have been reported to utilize glyphosate as a nutrient source or to break it down through pathways such as C–P lyase and glyphosate oxidoreductase. Environmental studies consistently show that glyphosate and its metabolite AMPA can be degraded under both field and microcosm conditions, with degradation rates influenced by soil type or nutrient availability.[29,34–37] Therefore, members of *Chloroflexota* were able to thrive and increase in abundance. The phylum *Desulfobacterota* increased in abundance over time, supporting the earlier visual observations (Fig. 3) that suggested glyphosate initially inhibited the growth of sulfate-reducing bacteria. *Desulfobacterota* are known to include slow-growing organisms that also typically inhabit the anaerobic, sulfate-rich zones at the bottom of Winogradsky columns.

To further explore the temporal changes of microbial taxa within the microbial communities, we analyzed the log-transformed relative abundances of the 40 most prominent families, grouped by their respective phyla (Fig. 6). At the family level, members of *Anaerolineaceae* from the phylum *Chloroflexota* showed continuous growth over time, supporting the proposed hypothesis that the MESIF material may

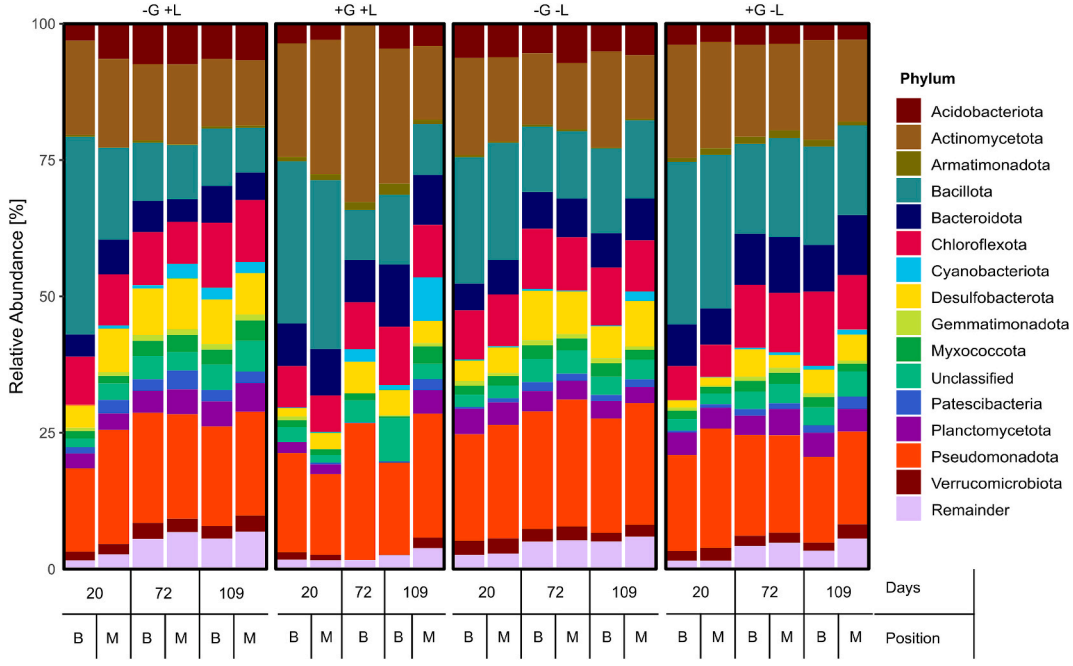

Fig. 5. Overview of the relative abundance of the 15 most abundant phyla detected in the Winogradsky columns. Conditions -G+L, +G+L, -G-L, and +G-L are shown from left to right for days 20, 72, and 109, with data collected from MESIF pieces positioned at the bottom (B) and middle (M) levels within the columns.

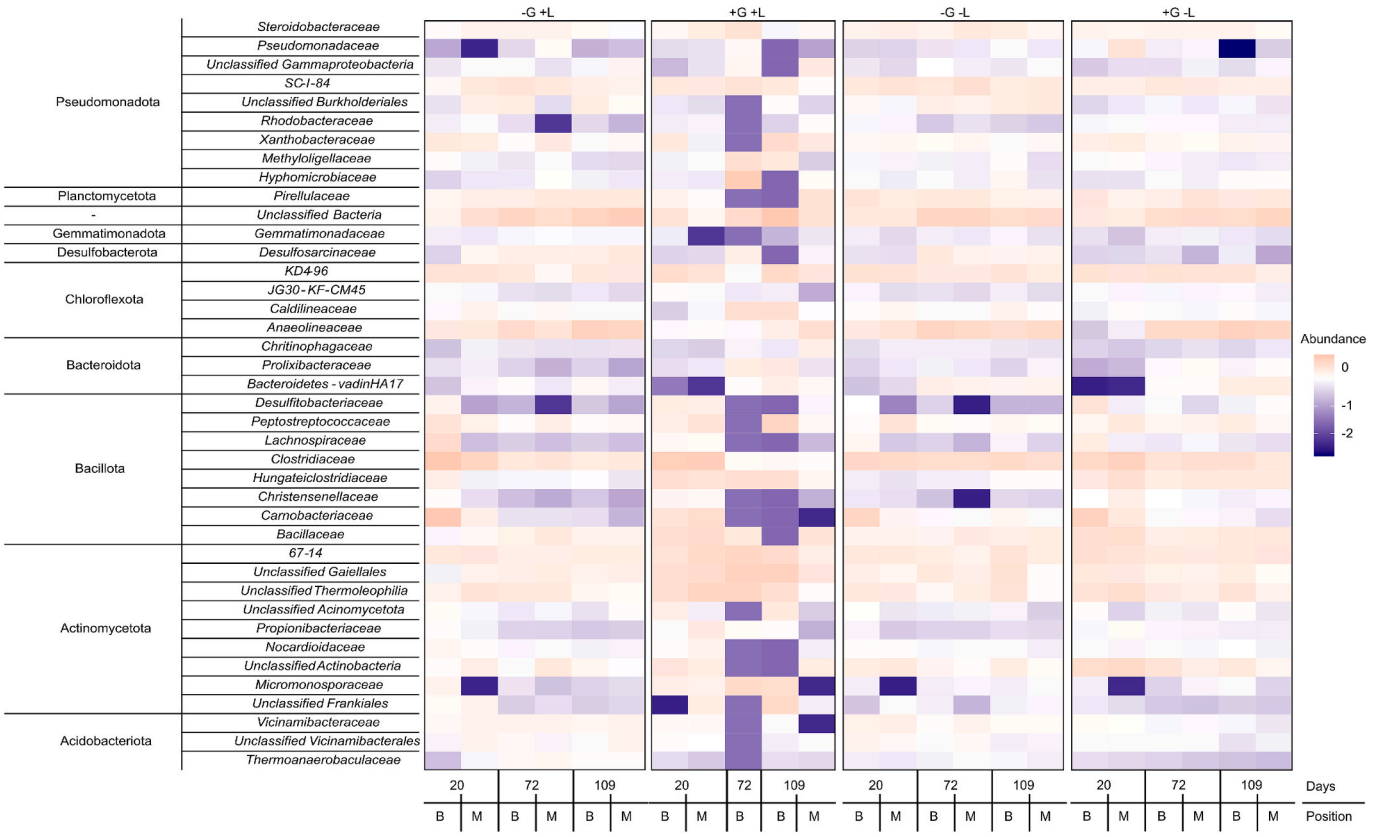

Fig. 6. Heatmap showing the log-transformed relative abundances of the 40 most prominent families, grouped by their respective phyla. Positive log10 fold changes are shown in red, while negative values are displayed in blue. Conditions -G+L, +G+L, -G-L, and +G-L are presented from left to right for days 20, 72, and 109, with data from MESIF pieces positioned at the bottom and middle levels. (For interpretation of the references to colour in this figure legend, the reader is referred to the web version of this article.)

positively influence their growth. Notably, the +G+L condition showed the highest compositional deviation from the other treatments, emphasizing the pronounced combined influence of glyphosate and light on the microbial community. These findings highlight the complex interactions between glyphosate, light, and microbial community dynamics, demonstrating how environmental factors drive shifts in microbial diversity and structure over time.

While a full functional analysis would require metagenomic sequencing, the observed taxonomic shifts allow us to formulate hypotheses about microbial pathways that may be affected by glyphosate treatment. Glyphosate resistance in bacteria can arise through mutations in the EPSPS gene (*aroA*), increased EPSPS activity via overexpression or gene amplification, or degradation of glyphosate as a nutrient source. [29] The best characterized degradation pathway is the C–P lyase system, which enables phosphorus acquisition from glyphosate, typically under phosphorus limitation, while a less common route involves glyphosate oxidoreductase (GOX), an oxygen-dependent cleavage reaction that has occasionally been reported under prolonged exposure. [29] In our study, several phyla decreased under glyphosate treatment, including *Desulfobacterota*, *Patescibacteria*, *Chloroflexota*, and *Acidobacteriota*, consistent with sensitivity to EPSPS inhibition and limited capacity for glyphosate degradation. *Desulfobacterota*, which include sulfate-reducing taxa, appeared initially suppressed, possibly reflecting disruption of redox cycling as reported previously.[29] By contrast, *Bacillota* increased under glyphosate, in line with previous findings that *Bacillus* spp. harbor phosphonate degradation pathways.[38] Similarly, *Bacteroidota* also increased in abundance, although their direct involvement in glyphosate metabolism remains unclear. Taken together, these patterns suggest that glyphosate exposure selectively suppressed some microbial groups while favoring others with potential tolerance or degradation capabilities. While 16S data alone cannot resolve the underlying molecular pathways, the observed shifts are consistent with established glyphosate resistance and degradation strategies.

3.5. Shifts in microbial taxa in response to glyphosate and light

To further explore the impact of glyphosate on microbial communities, we conducted differential abundance tests using bias-corrected compositional analysis (ANCOM-BC).[20] Genera showing significant changes ($p < 0.05$) under the -G-L, +G-L, and +G+L conditions were visualized as a heatmap based on their log-fold change (Fig. 7). Since the analysis identified a total of 185 differentially abundant taxa (Table S1), only the 20 with the highest and lowest log-fold changes are shown.

Overall, exposure to glyphosate led to significant shifts in microbial abundance, and light was also shown to influence the microbiome composition. Specifically, members of an unclassified genus within the *Weeksellaceae* family were enriched only in the presence of glyphosate, particularly under dark conditions (+G-L, Fig. 7). Previous studies have shown that members of this family can degrade glyphosate in contaminated soils,[39] suggesting that this novel genus may also have the capacity to degrade glyphosate.

A similar trend was observed for novel genera within the families *Anaerovoracaceae* and *Christensenellaceae*, which were significantly enriched only under glyphosate-treated conditions (+G-L and +G+L, Fig. 7). Notably, *Christensenellaceae* have already been shown to increase in abundance in rat microbiomes following glyphosate exposure,[40] whereas members of *Anaerovoracaceae* have not yet been reported to degrade glyphosate. Additionally, several species within the genus *Clostridium* were enriched in the presence of glyphosate. Since *Clostridium* is known to be resistant to glyphosate, its increased abundance

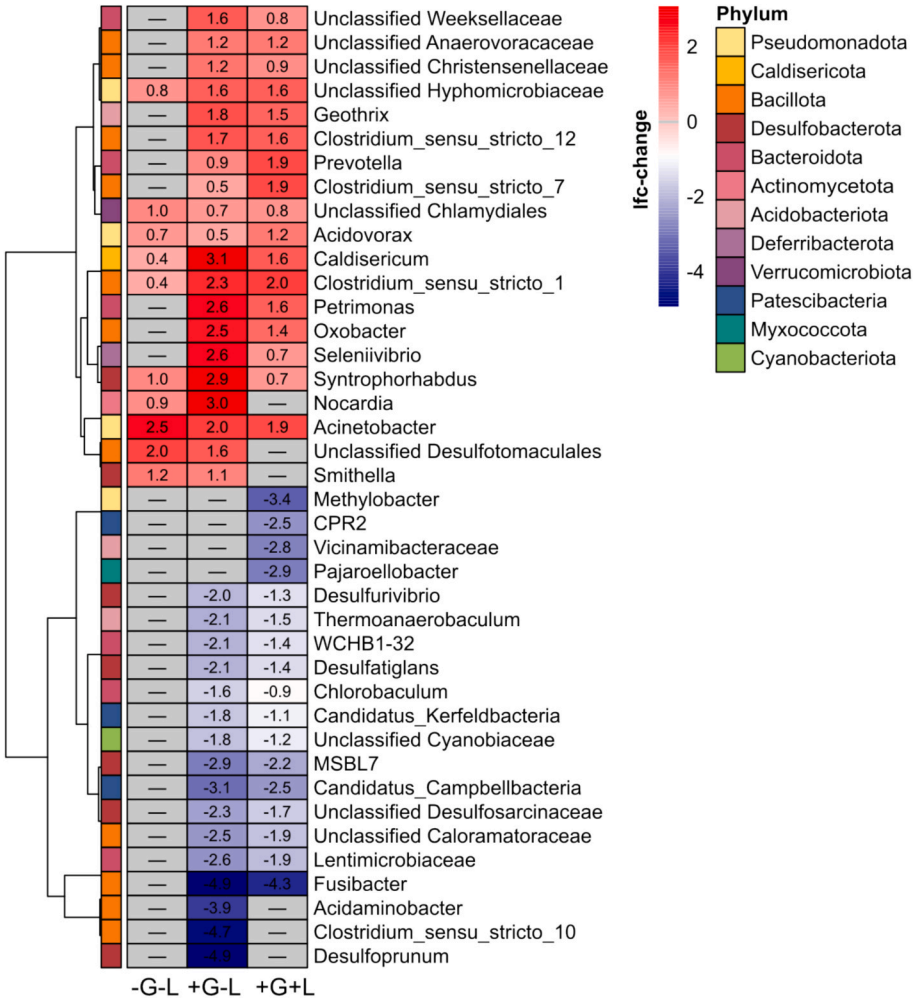

Fig. 7. Differentially abundant taxa based on bias-corrected microbiome composition analysis. The log fold change for the three displayed conditions (-G-L, +G-L, +G+L) is calculated relative to the reference condition (-G+L) at the genus level. The corresponding phyla are indicated by colored boxes to the left of the data columns. Significant positive changes are shown in red, while negative changes are shown in blue ($p < 0.05$). The dendrogram represents the phylogenetic relationships between the taxa. (For interpretation of the references to colour in this figure legend, the reader is referred to the web version of this article.)

may not be due to degradation potential but rather its ability to survive and coexist under glyphosate exposure.[41] Furthermore, the enrichment of the three mentioned genera (*Unclassified Anaerovoracaceae*, *Christensenellaceae*, and *Clostridium*), all belonging to the phylum *Bacillota*, aligns with the earlier hypothesis that *Bacillota* members may thrive under glyphosate exposure (Fig. 5, Fig. 6), indicating a potential role in glyphosate degradation.

Closer examination of taxa abundance revealed that the genera *Geothrix*, *Prevotella*, *Petrimonas*, *Oxobacter*, and *Seleniivibrio* were also significantly enriched in the presence of glyphosate (+G-L, +G+L, Fig. 7). *Geothrix* is well-studied for its iron-reducing capabilities, but no evidence exists for its involvement in glyphosate degradation. Interestingly, *Prevotella*, which has previously been shown to decrease under glyphosate exposure,[38] was enriched in our study under glyphosate-treated conditions. This raises the question of whether *Prevotella* might have a mechanism for tolerating low glyphosate concentrations.

Furthermore, glyphosate exposure influenced the enrichment of specific anaerobic and sulfur-reducing microbes, such as the genus *Caldisericum*, which was enriched under all glyphosate-treated conditions, particularly in the absence of light (+G-L, Fig. 7). While the only known member of this genus is capable of degrading sulfur compounds, its metabolic pathways remain poorly understood. Furthermore, under dark conditions, anaerobic genera such as *Petrimonas*, *Oxobacter*, *Seleniivibrio*, *Syntrophorhabdus*, *Desulfotomaculales*, and *Smithella* were enriched. None of these genera have been reported as glyphosate degraders, and their increased abundance may instead reflect tolerance to glyphosate exposure or indirect ecological interactions with other community members.

The +G-L columns, being shielded from light, showed no algal growth in their upper regions, as evidenced by the lack of green coloration on the inner surface of the columns (Fig. 3D). As a result, an oxygen gradient is unlikely to have developed within the column, which plausibly explains the increased enrichment of anaerobic taxa observed in comparison to the illuminated columns. Interestingly, while the genus *Acinetobacter*, widely recognized for its glyphosate-degrading potential, was identified as significantly different, the highest log-fold change occurred in the absence of both glyphosate and light (Fig. 7, -G-L, log-fold change of 2.5 compared to -G+L and +G+L). This pattern may reflect strain-level variability, since not all Acinetobacter species harbor the relevant degradation pathways. The ecological context may also play a role, as phosphonate utilization pathways such as the C–P lyase pathway are most advantageous under phosphate-limited conditions, [42] whereas in our columns other taxa, particularly members of the *Bacillota* phylum, may have been more effective competitors under glyphosate exposure.

To further examine the temporal enrichment of the previously

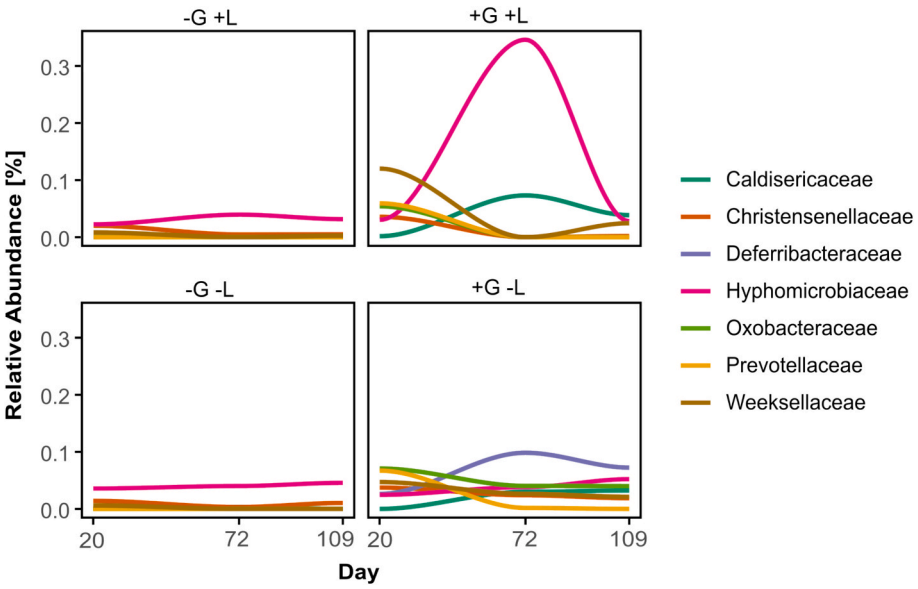

Fig. 8. Relative Abundances for enriched families in presence of glyphosate. Each plot represents one condition (-G+L, +G+L, -G-L and +G-L) and the lines are the respective families plotted based on the relative abundance referring to the total community. The longitudinal progression indicates the abundance on day 20, 72 and 109, respectively.

mentioned microbial groups, we analyzed the relative abundances of selected taxa at the family level to identify clear shifts over time. A consistent pattern emerged from the longitudinal analysis: key microbial families were enriched exclusively in the presence of glyphosate and were absent when glyphosate was not present (Fig. 8).

4. Conclusion

In summary, we present a method for spatiotemporal sampling of benthic microbial communities in Winogradsky columns as model ecosystems to study the effect of glyphosate on soil bacteria and to investigate whether glyphosate-degrading taxa are enriched. This was achieved by suspending MESIF pieces at fixed heights within the columns using steel frames. Columns were prepared with glyphosate and light, alongside appropriate controls for both factors. After a defined incubation period, the MESIF-holding frames were retrieved, and DNA was extracted and sequenced from the MESIF pieces.

The observed stratification patterns within the columns provided early visual evidence of glyphosate's impact on microbial communities. Columns treated with glyphosate developed stratification later than untreated controls and showed fewer signs of iron-oxidizing and sulfate-reducing bacteria. We hypothesize that glyphosate's metal-chelating properties may have reduced iron availability, thereby limiting the growth of iron-dependent taxa. This opens an avenue for future investigations to clarify whether metal chelation is indeed a driving factor in these community shifts.

Sequencing results further revealed a strong correlation between glyphosate presence and shifts in microbial community composition, with enrichment of taxa that appear able to tolerate or metabolize this compound. While these data highlight clear associations, they do not establish causality. The precise mechanisms of microbial adaptation to glyphosate therefore remain unresolved, opening opportunities for future functional studies targeting the suspected glyphosate degraders identified here.

While certain taxa show potential for glyphosate degradation, further research is needed to unravel the underlying metabolic pathways and ecological implications of these microbial shifts. Although this study was conducted with two replicates per condition and timepoint, the use of standardized MESIF matrices ensured reproducibility and spatial resolution, establishing a robust workflow that can be expanded in future studies with larger replication. The methods established here can be adapted to other environments. Extended variants of the MESIF-loaded frames may be embedded into soils or aquatic sediments with glyphosate contamination to study microbial community dynamics across different depths. This adaptability opens opportunities to investigate glyphosate impacts in natural and agricultural ecosystems, to deepen our understanding of complex microbial ecosystems and to even identify microbial taxa with potential for bioremediation.

Funding

This work was supported through the Helmholtz program "Materials Systems Engineering" under the topic "Adaptive and Bioinstructive Materials Systems" (43.33.11).

Declaration of competing interest

The authors declare no conflict of interest.

Acknowledgements

The authors thank Anna Edinger, Julia Weißer, and Saskia Gimmel for experimental help. We would like to thank the NABU group Hambrücken, in particular its chairman Mr. Franz Debatin, for their friendly and very helpful support during the sediment sampling. We thank Simone Weigel and David Zellmer for helping fabricate the MESIF. We also thank Marius Stöckle for his suggestions on potential links between glyphosate and antibiotics producers.

Appendix A. Supplementary data

Supplementary data to this article can be found online at https://doi.org/10.1016/j.ymeth.2025.10.009.

Data availability

Illumina raw sequencing data is available on http://www.ncbi.nlm.nih.gov/bioproject/1272562. Other data available upon reasonable request from the corresponding author.

References

[1] M.E. Richmond, Glyphosate: a review of its global use, environmental impact, and potential health effects on humans and other species, J. Environ. Stud. Sci. 8 (2018) 416–434, https://doi.org/10.1007/s13412-018-0517-2.

[2] M. Hagner, J. Mikola, I. Saloniemi, K. Saikkonen, M. Helander, Effects of a glyphosate-based herbicide on soil animal trophic groups and associated ecosystem functioning in a northern agricultural field, Sci. Rep. 9 (2019) 8540, https://doi.org/10.1038/s41598-019-44988-5.

[3] Marques, J.G.C.; Veríssimo, K.J.S.F., B.S.; Ferreira, S.R.M.; Montenegro, S.M. G.L..; Motteran, F., Glyphosate: A Review on the Current Environmental Impacts from a Brazilian Perspective, Bull. Environ. Contam. Toxicol. 107 (2021) 385-397. doi: 10.1007/s00128-021-03295-4.

[4] B.S. Ojelade, O.S. Durowoju, P.O. Adesoye, S.W. Gibb, G.-I. Ekosse, Review of Glyphosate-based Herbicide and Aminomethylphosphonic Acid (AMPA): Environmental and Health Impacts, Appl. Sci. 12 (2022) 8789, https://doi.org/10.3390/app12178789.

[5] G.A. Zavarzin, Winogradsky and modern microbiology, Microbiology 75 (2006) 501–511, https://doi.org/10.1134/S0026261706050018.

[6] Kearns, E.A.; Folsome, C.E., Measurement of biological activity in materially closed microbial ecosystems, BioSyst. 14 (1981) 205-209. doi:doi:10.1016/0303-2647(81)90069-1.

[7] L.M. de Jesús Astacioa, K.H. Prabhakara, Z. Li, H. Mickalide, S. Kuehn, Closed microbial communities self-organize to persistently cycle carbon, Proc. Natl. Acad. Sci. U.S.A. 118 (2021) e2013564118, https://doi.org/10.1073/pnas.2013564118.

[8] S.P. Weatherley, H.K. Laird, C.M. Gatley-Montross, S.B. Whorley, The Effects of Roundup™ on Benthic Microbial Assemblages, Ecologies 3 (2022) 557–569, https://doi.org/10.3390/ecologies3040041.

[9] D.J. Esteban, B. Hysa, C. Bartow-McKenney, Temporal and Spatial distribution of the Microbial Community of Winogradsky Columns, PLoS One 10 (2015) e0134588, https://doi.org/10.1371/journal.pone.0134588.

[10] Zoheir, A.E.; Meisch, L.; Martín, M.V.; Bickmann, C.; Kiselev, A.; Lenk, F.; Kaster, A.-K.; Rabe, K.S.; Niemeyer, C.M., Macroporous Silicone Chips for Decoding Microbial Dark Matter in Environmental Microbiomes, ACS Appl. Mater. Interfaces 14 (2022) 49592–49603. doi:doi:10.1021/acsami.2c15470.

[11] E. Bolyen, J.R. Rideout, M.R. Dillon, N.A. Bokulich, C.C. Abnet, G.A. Al-Ghalith, H. Alexander, E.J. Alm, M. Arumugam, F. Asnicar, et al., Reproducible, interactive, scalable and extensible microbiome data science using QIIME 2, Nat. Biotechnol. 37 (2019) 852–857, https://doi.org/10.1038/s41587-019-0209-9.

[12] B.J. Callahan, P.J. McMurdie, M.J. Rosen, A.W. Han, A.J.A. Johnson, S.P. Holmes, DADA2: High-resolution sample inference from Illumina amplicon data, Nat. Methods 13 (2016) 581–583, https://doi.org/10.1038/nmeth.3869.

[13] Katoh, K.; Misawa, K.; Kuma, K.i.; Miyata, T., MAFFT: a novel method for rapid multiple sequence alignment based on fast Fourier transform, Nucleic Acids Res. 30 (2002) 3059-3066. doi:10.1093/nar/gkf436.

[14] M.N. Price, P.S. Dehal, A.P. Arkin, FastTree 2 – approximately Maximum-Likelihood Trees for Large Alignments, PLoS One 5 (2010) e9490.

[15] Bisanz, J.E., qiime2R: Importing QIIME2 artifacts and associated data into R sessions. https://github.com/jbisanz/qiime2R, 2018 (accessed April 17).

[16] P.J. McMurdie, S. Holmes, phyloseq: an R Package for Reproducible Interactive Analysis and Graphics of Microbiome Census Data, PLoS One 8 (2013) e61217, https://doi.org/10.1371/journal.pone.0061217.

[17] Lahti, L.; Shetty, S.; al., e., Tools for microbiome analysis in R. http://microbiome.github.com/microbiome, 2018 (accessed April 17).

[18] N.A. Bokulich, B.D. Kaehler, J.R. Rideout, M. Dillon, E. Bolyen, R. Knight, G. A. Huttley, J. Gregory Caporaso, Optimizing taxonomic classification of marker-gene amplicon sequences with QIIME 2's q2-feature-classifier plugin, Microbiome 6 (2018) 90, https://doi.org/10.1186/s40168-018-0470-z.

[19] Robeson, M.S., II; O'Rourke, D.R.; Kaehler, B.D.; Ziemski, M.; Dillon, M.R.; Foster, J.T.; Bokulich, N.A., RESCRIPt: Reproducible sequence taxonomy reference database management, PLOS Comput. Biol. 17 (2021) e1009581. doi:10.1371/journal.pcbi.1009581.

[20] H. Lin, S.D. Peddada, Analysis of compositions of microbiomes with bias correction, Nat. Commun. 11 (2020) 3514, https://doi.org/10.1038/s41467-020-17041-7.

[21] M.L. Castrejon-Godinez, E. Tovar-Sanchez, L. Valencia-Cuevas, M.E. Rosas-Ramirez, A. Rodriguez, P. Mussali-Galante, Glyphosate Pollution Treatment and Microbial Degradation Alternatives, a Review, Microorganisms 9 (2021), https://doi.org/10.3390/microorganisms9112322.

[22] S. Bott, T. Tesfamariam, A. Kania, B. Eman, N. Aslan, V. Römheld, G. Neumann, Phytotoxicity of glyphosate soil residues re-mobilised by phosphate fertilisation, Plant Soil 342 (2011) 249–263, https://doi.org/10.1007/s11104-010-0689-3.

[23] D.A. Martinez, U.E. Loening, M.C. Graham, Impacts of glyphosate-based herbicides on disease resistance and health of crops: a review, Environ. Sci. Eur. 30 (2018) 2, https://doi.org/10.1186/s12302-018-0131-7.

[24] M.M. Newman, N. Lorenz, N. Hoilett, N.R. Lee, R.P. Dick, M.R. Liles, C. Ramsier, J. W. Kloepper, Changes in rhizosphere bacterial gene expression following glyphosate treatment, Sci. Total Environ. 553 (2016) 32–41, https://doi.org/10.1016/j.scitotenv.2016.02.078.

[25] J.G. Caporaso, J. Kuczynski, J. Stombaugh, K. Bittinger, F.D. Bushman, E. K. Costello, N. Fierer, A.G. Peña, J.K. Goodrich, J.I. Gordon, et al., QIIME allows analysis of high-throughput community sequencing data, Nat. Methods 7 (2010) 335–336, https://doi.org/10.1038/nmeth.f.303.

[26] J.G. Kers, E. Saccenti, The Power of Microbiome Studies: some Considerations on which Alpha and Beta Metrics to use and how to Report results, Front. Microbiol. 12 (2022) 796025, https://doi.org/10.3389/fmicb.2021.796025.

[27] I. Cassol, M. Ibañez, J.P. Bustamante, Key features and guidelines for the application of microbial alpha diversity metrics, Sci. Rep. 15 (2025) 622, https://doi.org/10.1038/s41598-024-77864-y.

[28] E. Schonbrunn, S. Eschenburg, W.A. Shuttleworth, J.V. Schloss, N. Amrhein, J. N. Evans, W. Kabsch, Interaction of the herbicide glyphosate with its target enzyme 5-enolpyruvylshikimate 3-phosphate synthase in atomic detail, Proc. Natl. Acad. Sci. U. S. A. 98 (2001) 1376–1380, https://doi.org/10.1073/pnas.98.4.1376.

[29] R. Hertel, J. Gibhardt, M. Martienssen, R. Kuhn, F.M. Commichau, Molecular mechanisms underlying glyphosate resistance in bacteria, Environ. Microbiol. 23 (2021) 2891–2905, https://doi.org/10.1111/1462-2920.15534.

[30] Y. Yuan, Z. Zhou, Y. Zhan, X. Ke, Y. Yan, M. Lin, P. Li, S. Jiang, J. Wang, W. Lu, A Highly Glyphosate-Resistant EPSPS Mutant from Laboratory Evolution, Appl. Sci. 12 (2022), https://doi.org/10.3390/app12115723.

[31] M. Giannakara, V.L. Koumandou, New Insights on the Glyphosate-Degrading Enzymes C-P Lyase and Glyphosate Oxidoreductase based on Bioinformatics, Bacteria 3 (2024) 314–329, https://doi.org/10.3390/bacteria3040021.

[32] T. Yamada, Y. Sekiguchi, Cultivation of Uncultured *Chloroflexi* Subphyla: significance and Ecophysiology of Formerly Uncultured *Chloroflexi* 'Subphylum I' with Natural and Biotechnological Relevance, Microbes Environ. 24 (2009) 205–216, https://doi.org/10.1264/jsme2.ME09151S.

[33] T. Nunoura, M. Hirai, M. Miyazaki, H. Kazama, H. Makita, H. Hirayama, Y. Furushima, H. Yamamoto, H. Imachi, K. Takai, Isolation and Characterization of a Thermophilic, Obligately Anaerobic and Heterotrophic Marine *Chloroflexi* Bacterium from a *Chloroflexi*-dominated Microbial Community Associated with a Japanese Shallow Hydrothermal System, and Proposal for *Thermomarinilinea lacunofontalis* gen. nov., sp. nov, Microbes Environ. 28 (2013) 228–235, https://doi.org/10.1264/jsme2.ME12193.

[34] S. Singh, V. Kumar, J. Singh, Kinetic study of the biodegradation of glyphosate by indigenous soil bacterial isolates in presence of humic acid, Fe(III) and Cu(II) ions, J. Env. Chem. Eng. 7 (2019), https://doi.org/10.1016/j.jece.2019.103098.

[35] B. Wimmer, A. Langarica-Fuentes, E. Schwarz, S. Kleindienst, C. Huhn, H. Pagel, Mechanistic modeling indicates rapid glyphosate dissipation and sorption-driven persistence of its metabolite AMPA in soil, J. Environ. Qual. 52 (2023) 393–405, https://doi.org/10.1002/jeq2.20437.

[36] M.I. Morales-Olivares, M.L. Castrejon-Godinez, P. Mussali-Galante, E. Tovar-Sanchez, H.A. Saldarriaga-Norena, A. Rodriguez, Characterization of Glyphosate Resistance and Degradation Profile of Caballeronia zhejiangensis CEIB S4-3 and Genes involved in its Degradation, Microorganisms 13 (2025), https://doi.org/10.3390/microorganisms13030651.

[37] Y. Chen, W.J. Chen, Y. Huang, J. Li, J. Zhong, W. Zhang, Y. Zou, S. Mishra, P. Bhatt, S. Chen, Insights into the microbial degradation and resistance mechanisms of glyphosate, Environ. Res. 215 (2022) 114153, https://doi.org/10.1016/j.envres.2022.114153.

[38] L. Walsh, C. Hill, R.P. Ross, Impact of glyphosate (RoundupTM) on the composition and functionality of the gut microbiome, Gut Microbes 15 (2023) 2263935, https://doi.org/10.1080/19490976.2023.2263935.

[39] Zhang, W.; Li, J.; Zhang, Y.; Wu, X.; Zhou, Z.; Huang, Y.; Zhao, Y.; Mishra, S.; Bhatt, P.; Chen, S., Characterization of a novel glyphosate-degrading bacterial species, Chryseobacterium sp. Y16C, and evaluation of its effects on microbial communities in glyphosate-contaminated soil, J. Hazard. Mater. 432 (2022) 128689. doi:doi:10.1016/j.jhazmat.2022.128689.

[40] R. Mesnage, S. Panzacchi, E. Bourne, C.A. Mein, M.J. Perry, J. Hu, J. Chen, D. Mandrioli, F. Belpoggi, M.N. Antoniou, Glyphosate and its formulations Roundup Bioflow and RangerPro alter bacterial and fungal community composition in the rat caecum microbiome, Front. Microbiol. 13 (2022) 888853, https://doi.org/10.3389/fmicb.2022.888853.

[41] Rueda-Ruzafa, L.; Cruz, F.; Roman, P.; Cardona, D., Gut microbiota and neurological effects of glyphosate, Neurotoxicology 75 (2019) 1-8. doi:doi:10.1016/j.neuro.2019.08.006.

[42] A.V. Sviridov, T.V. Shushkova, I.T. Ermakova, E.V. Ivanova, D.O. Epiktetov, A. A. Leontievsky, Microbial degradation of glyphosate herbicides (Review), Appl. Biochem. Microbiol. 51 (2015) 188–195, https://doi.org/10.1134/s0003683815020209.